Supporting Information for

Ion-Selective Electrodes with Unusual Response Functions: Simultaneous Formation of Ionophore–Primary Ion Complexes with Different Stoichiometries

Masafumi Miyake,[1] Li D. Chen,[1] Gianluca Pozzi,[2] and Philippe Bühlmann[*,1]*

[1]Department of Chemistry, University of Minnesota, 207 Pleasant St. SE, Minneapolis MN 55455, USA, [2]CNR-Istituto di Scienze Tecnologie Molecolari, via Golgi 19, 20133, Milano, Italy.

Email Address: buhlmann@umn.edu

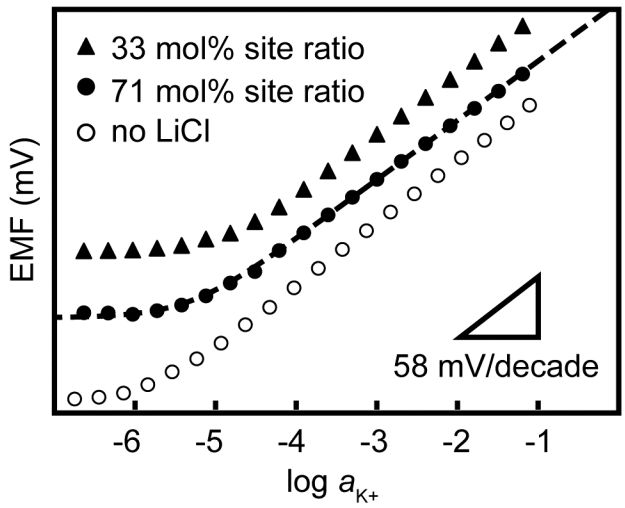

Figure S1. Potentiometric K^+ responses of an ISE based on a perfluoroperhydrophenanthrene membrane doped with ionophore (**1**, 2.0 mmol L^{-1}) and anionic sites at a site-to-ionophore ratio of 71 mol % (filled circles) or 33 mol % (diamonds) in the presence of 0.5 mol L^{-1} Li^+. For comparison, the K^+ response curve for a 71 mol % membrane in the absence of interfering ions is shown as well (open circles). The response of the 71 mol % membrane was fitted (broken line) with the model described in the text and the following parameters: $K_{ex} = 10^{1.41}$, $K_{KL} = 10^{15.1}$, $K_{KL2} = 10^{6.0}$, $K_{LiL} = 10^{11.7}$, and $K_{LiL2} = 10^{6.2}$.

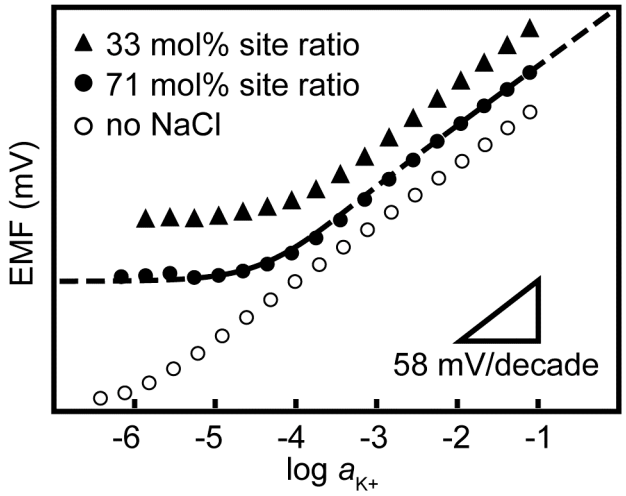

Figure S2. Potentiometric K^+ responses of an ISE based on a perfluoroperhydrophenanthrene membrane doped with ionophore (**1**, 2.0 mmol L^{-1}) and anionic sites at a site-to-ionophore ratio of 71 mol % (filled circles) or 33 mol % (diamonds) in the presence of 10 mol L^{-1} Na^+. For comparison, the K^+ response curve for a 71 mol % membrane in the absence of interfering ions is shown as well (open circles). The response of the 71 mol % membrane was fitted (broken line) with the model described in the text and the following parameters: $K_{ex} = 10^{1.00}$, $K_{KL} = 10^{15.1}$, $K_{KL2} = 10^{5.9}$, $K_{NaL} = 10^{14.0}$, and $K_{NaL2} = 10^{6.4}$.

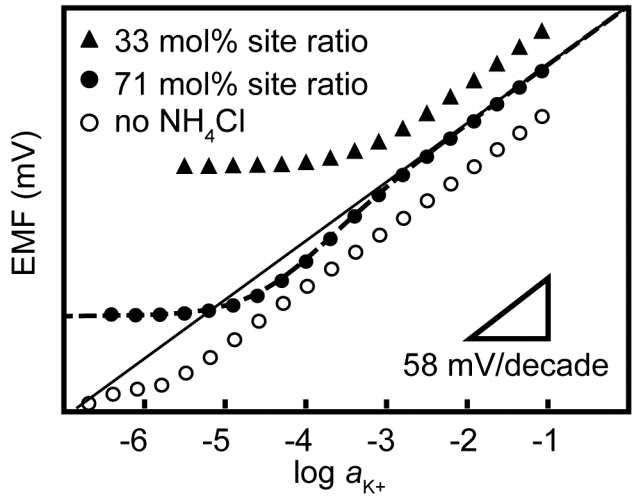

Figure S3. Potentiometric K^+ responses of an ISE based on a perfluoroperhydrophenanthrene membrane doped with ionophore (**1**, 2.0 mmol L^{-1}) and anionic sites at a site-to-ionophore ratio of 71 mol % (filled circles) or 33 mol % (diamonds) in the presence of 2.0 mol L^{-1} NH_4^+. For comparison, the K^+ response curve for a 71 mol % membrane in the absence of interfering ions is shown as well (open circles). The response of the 71 mol % membrane was fitted (broken line) with the model described in the text and the following parameters: $K_{ex} = 10^{-0.55}$, $K_{KL} = 10^{15.1}$, $K_{KL2} = 10^{6.0}$, $K_{NH4L} = 10^{12.9}$, and $K_{NH4L2} = 10^{7.0}$.

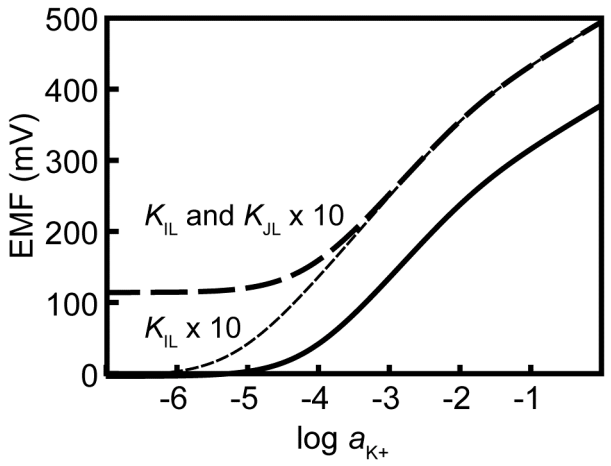

Figure S4. Predicted K^+ responses of an ISE based on ionophore (**1**, 2.0 mmol L^{-1}) and anionic sites at a site-to-ionophore ratio of 71 mol % in the presence of 1 mmol L^{-1} Cs^+, as calculated with the model described in the text. Solid line: $K_{ex}= 10^{-0.55}$, $K_{KL}= 10^{15.1}$, $K_{KL2} = 10^{6.0}$, $K_{CsL} = 10^{11.5}$, and $K_{CsL2} = 10^{8.3}$ (identical with broken line fit of Figure 3). Thin broken line: Same parameters as for solid line, except for a ten times larger value of K_{KL}. Thick dashed line: Same parameters as for solid line, except for a ten times larger values of K_{KL} and K_{CsL}.

Width of the K^+ Activity Range in Which a Super-Nernstian Response is Observed

Going from low to higher activities of K^+ in a background of constant activity of Cs^+ or NH_4^+ (see filled circles and broken lines in Figure 3 of the main paper and Figure S3 of the Supporting Information), the EMF is at first constant and is dominated by the interfering ion (i.e., Cs^+ or NH_4^+). This is followed at somewhat higher K^+ activities by the onset of the super-Nernstian response. The onset point is characterized by the formation of the complex JL^+ and disappearance of IL^+ (see Figures 4 and 5 in the main paper). The K^+ activity at the onset of the super-Nernstian response can be obtained by solving the set of equations 2 to 6 a first time for $[IL]$ as a function of $[L]$, and a second time for $[JL]$ as a function of $[L]$. The two functions are too long to reproduce here, but knowing that at the onset of the super-Nernstian response $[IL] = [JL]$, the two functions for $[IL]$ and $[JL]$ can be set equal to one another, and the resulting equation is solved for $a_{I,aq}$. This gives the onset of the super-Nernstian response as $a_{J,aq} K_{JL} \left(K_{ex} K_{IL}\right)^{-1}$, which is represented in Figure S5 as a_1.

The end of the super-Nernstian response range and the onset of the Nernstian response range (represented in Figure S5 as a_2) is characterized by the formation of the complexes IL_2^+ and the disappearance of JL_2^+ in the sensing membrane. The onset point of the Nernstian response can be obtained by first solving the set of equations 2 to 6 for $[IL_2]$ as a function of $[L]$, and a second time for $[JL_2]$ as a function of $[L]$. The two functions are too long to reproduce here, but knowing that at the onset of the Nernstian response $[IL_2] = [JL_2]$, the two functions for $[IL_2]$ and $[JL_2]$ can be set

equal to one another, and the resulting equation is solved for $a_{\mathrm{I,aq}}$. This gives the onset of the Nernstian response as $a_{\mathrm{J,aq}} K_{\mathrm{JL}} K_{\mathrm{JL2}} \left(K_{\mathrm{ex}} K_{\mathrm{IL}} K_{\mathrm{IL2}}\right)^{-1}$.

It follows that the width of the super-Nernstian response in the plot of the EMF versus the logarithm of the K^+ activity is given by:

$$\log \frac{a_{\mathrm{J,aq}} K_{\mathrm{JL}} K_{\mathrm{JL2}}}{K_{\mathrm{ex}} K_{\mathrm{IL}} K_{\mathrm{IL2}}} - \log \frac{a_{\mathrm{J,aq}} K_{\mathrm{JL}}}{K_{\mathrm{ex}} K_{\mathrm{IL}}}$$

which can be simplified to $\log\left(K_{\mathrm{JL2}}/K_{\mathrm{IL2}}\right)$.

A third point that is characteristic of the response curve can be obtained by the extrapolation of the Nernstian response down to the constant value of the EMF that is observed for very low activities of K^+ (i.e., when the EMF is governed by the interfering ion alone; labeled with a_3 in Figure S5). For a system in which $[\mathrm{L}] << [\mathrm{IL}], [\mathrm{IL_2}], [\mathrm{JL}], [\mathrm{JL_2}]$, this third point is found at:

$$a_{\mathrm{I,aq}} = \frac{a_{\mathrm{J,aq}} K_{\mathrm{JL}} K_{\mathrm{IL2}}}{K_{\mathrm{ex}} K_{\mathrm{IL}} K_{\mathrm{JL2}}}$$

This can be shown by (1) applying equations 2 and 3 for i = I and solving for $[\mathrm{I}]$, (2) applying equations 2 and 3 for i = J and solving for $[\mathrm{J}]$, (3) solving equation 6 for $[\mathrm{J}]$, (4) setting the two expressions for $[\mathrm{J}]$ from steps 2 and 3 equal to one another and solving for $[\mathrm{I}]$, (5) setting the two expressions for $[\mathrm{I}]$ from steps 1 and 4 equal to one another and solving for $a_{\mathrm{I,aq}}$, and (6) simplifying the resulting expression using $[\mathrm{IL}] \approx [\mathrm{JL}]$ and $[\mathrm{IL_2}] \approx [\mathrm{JL_2}]$. This is based on the fact that the expression from step 1 gives the concentration of I in the sensing membrane on any point on the linear section of the (Nernstian) primary ion response (as if there were no interfering ion present at all), while

the expression from step 5 gives the concentration of I^+ in the sensing membrane as found when the activity of I^+ in the aqueous sample is small, and complexes of J^+ dominate in the sensing membrane. Note that the two equations $[IL] \approx [JL]$ (where $[IL]$ is the concentration of IL^+ in a membrane exposed to aqueous solutions containing only I^+, and $[JL]$ is the concentration of JL^+ in a membrane in which complexes of J^+ dominate) and $[IL_2] \approx [JL_2]$ (where $[IL_2]$ is the concentration of IL_2^+ in a membrane exposed to aqueous solutions containing only I^+, and $[JL_2]$ is the concentration of JL_2^+ in a membrane in which complexes of J^+ dominate) are only true when $[L] << [IL],[IL_2],[JL],[JL_2]$. The expression $a_{I,aq} = \frac{a_{J,aq} K_{JL} K_{IL2}}{K_{ex} K_{IL} K_{JL2}}$ shows that the position of this third characteristic point on the log $a_{I,aq}$ axis depends on the same parameters as the width of the activity range in which a super-Nernstian response is observed.

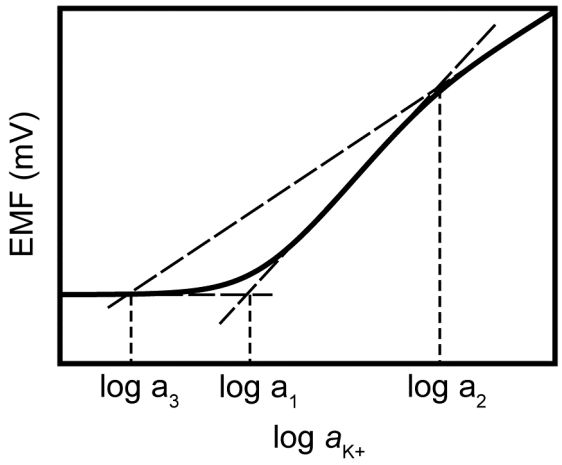

Figure S5. Definition of a_1, a_2, and a_3 as used in the above discussion of the super-Nernstian response range. The labels a_1 and a_2 refer to the onset and end of the super-Nernstian response, respectively, and a_3 is given by the extrapolation of the Nernstian response down to the constant value of the EMF.

As shown above, the width of the K^+ activity range in which a super-Nernstian response is observed is given by $\log\left(K_{\mathrm{JL2}}/K_{\mathrm{IL2}}\right)$ and does not seem to depend on the concentration of ionic sites. Figure S6 illustrates the latter. It shows the K^+ response as calculated for membranes with ionic site-to-ionophore ratios in the range from 50.0500 to 99.9995 mol % (from top to bottom) and parameters otherwise identical with those used for the fit of the K^+ response in the presence of 1 mmol L^{-1} Cs^+, as shown in Figure 3 of the manuscript. The figure illustrates that for intermediate ionic site-to-ionophore ratios the width of the super-Nernstian response does indeed not depend on the ionic site-to-ionophore ratio. However, as the ionic site-to-ionophore ratio approaches very closely either 50 or 100 mol %, the slope in the super-Nernstian response range decreases gradually and becomes indistinguishable from the Nernstian response. This is readily explained by the dominance of 2:1 and 1:1 complexes at 50 or 100 mol % ionic sites, respectively.

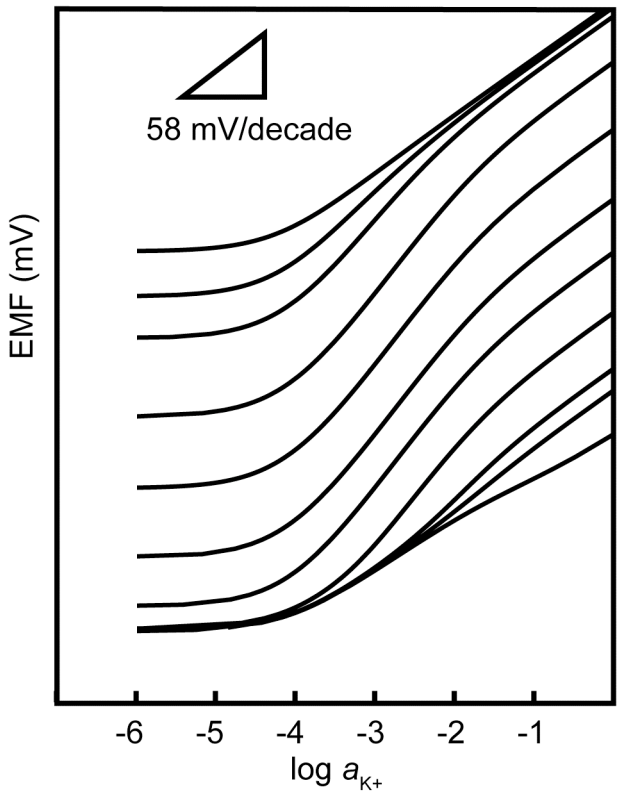

Figure S6. Calculated potentiometric K^+ responses of ISEs doped with an ionophore (2.0 mmol L^{-1}) and anionic sites at site-to-ionophore ratios of 50.05, 50.20, 50.50, 52.50, 60.00, 80.00, 95.00, 99.50, 99.95, 99.98, and 99.9995 mol % (from top to bottom) in the presence of 1 mmol L^{-1} Cs^+ in the sample. All responses were calculated with the model described in the text and the following parameters: $K_{ex}= 10^{-2.51}$, $K_{KL}= 10^{15.1}$, $K_{KL2} = 10^{6.0}$, $K_{CsL} = 10^{11.5}$, and $K_{CsL2} = 10^{8.3}$, as also used for the fit shown in Figure 3.

Sub-Nernstian Responses and Potential Dips

The EMF response model accounting for the coexistence in ISE membranes of 1:1 and 1:2 complexes of the target ion (as well as 1:1 and 1:2 complexes of the interfering ion), as developed in the body of the associated paper, is very general in nature. Therefore, it can also be used to predict EMF responses of ISEs other than those exhibiting super-Nernstian responses. Depending on the stabilities of the 1:1 and 1:2 complexes of the primary and interfering ions, not only super-Nernstian but also Nernstian and sub-Nernstian responses (see Figure S7, curve A) as well as potential dips (Figure 7, curve B) are predicted. (For comparison, Figure S7 shows as curve C the fit of the experimentally observed K^+ response shown also in Figure 3.)

One trivial example for the application of this response model results when for each type of ion only one complex has a substantial stability, and all other stability constants are exceedingly small. In this case, the predicted EMF response curves are identical to those predicted with the Nikolskii-Eisenman equation.

An example of a theoretically predicted sub-Nernstian response region is shown as curve A in Figure S7. For this example, it was assumed that the interfering ion does not interact with the ionophore at all, as it is typically expected, e.g., for tetraalkylammonium ions. Note the similarity of, on one hand, the hypothetical binding constants K_{KL} and K_{KL2} used for this theoretical EMF response calculation and, on the other hand, the K_{KL} and K_{KL2} *values* as experimentally determined for the fluorophilic ionophore **1**.

The experimentally determined value of K_{KL} is only 20 times smaller and the experimentally determined value of K_{KL2} *is only 40 times larger than the respective values used for the calculation of the hypothetical EMF response exhibiting the sub-Nernstian region. A very similar calculation was also performed* for an interfering ion that does not interact with the ionophore at all and the binding constants K_{KL} and K_{KL2} for the primary ion as experimentally determined for K^+ in this paper; in this case, the initial sub-Nernstian rise of the EMF is followed at higher primary ion activities by a nearly flat EMF response and at yet higher K^+ activities by the Nernstian response (not shown).

*The EMF response curve B of Figure S7 with a potential dip was also calculated for a set of parameters that seem very realistic. For the primary ion, the same binding constants were used as determined experimentally in this work for K^+ and ionophore **1**. For the interfering ion, the same value of the 1:1 binding constant (K_{JL})* was used as for the primary ion, and the value of K_{JL2} was chosen as 100 times smaller than for K_{KL2}.

We are not aware at this point of any experimental observations of sub-Nernstian responses or potential dips that need to be explained on the basis of the model described here. However, we believe that just as the super-Nernstian responses discussed in the main body of this paper too, sub-Nernstian responses and potential dips are probably relatively common but have been overlooked or misinterpreted in the past because they were not properly interpreted. It is all too easy to misinterpret such an effect as the result of transmembrane ion fluxes. Whenever a deviation of an EMF response

from the shape predicted by the Nikolskii-Eisenman equation is experimentally observed, both ion fluxes and the coexistance of complexes of differing stoichiometries (as discussed in this paper) should be considered as possible explanations.

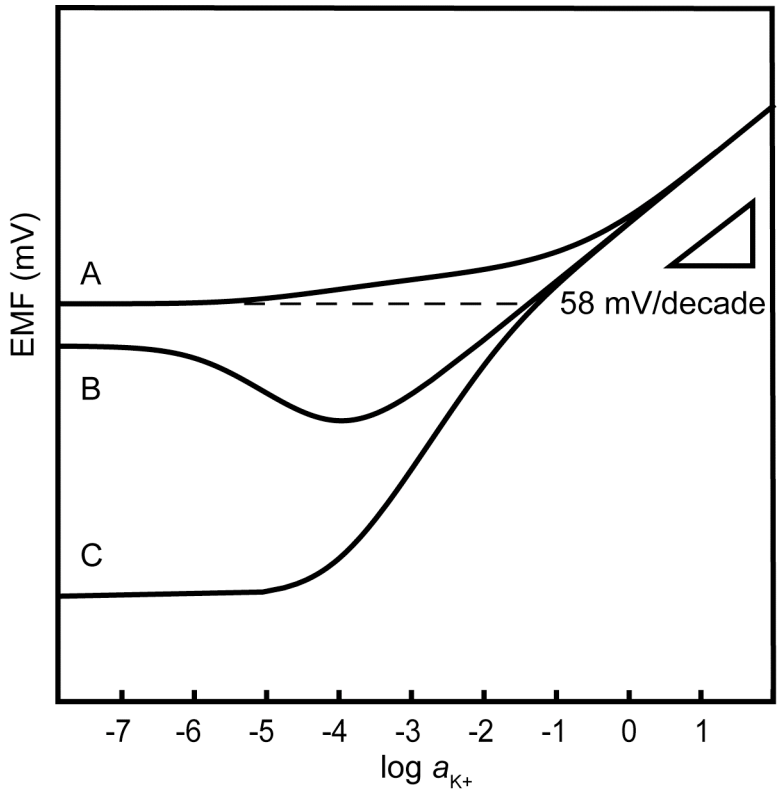

Figure S7. Calculated potentiometric K^+ responses of ISEs doped with an ionophore (2.0 mmol L^{-1}) and anionic sites at a site-to-ionophore ratio of 71 mol %: (A) For an aqueous sample containing 1 mmol L^{-1} of an interfering monocation that does not bind to the ionophore at all. $K_{ex}= 10^{-14.0}$, $K_{KL}= 10^{16.4}$, $K_{KL2}= 10^{4.4}$. (B) For an aqueous sample containing 1 mmol L^{-1} of an interfering monocation that binds to the ionophore with the same 1:1 binding constant as K^+ *(*$K_{JL}= 10^{15.1}$) but $K_{JL2}= 10^{4.0}$. Other parameters as for the fit in Figure 3: $K_{ex}= 10^{-2.51}$, $K_{KL}= 10^{15.1}$, $K_{KL2}= 10^{6.0}$. (C) Fit of K^+ response in the presence of 1 mmol L^{-1} Cs^+ as shown in Figure 3 ($K_{ex}= 10^{-2.51}$, $K_{KL}= 10^{15.1}$, $K_{KL2}= 10^{6.0}$). Curve A was shifted vertically with respect to curves B and C to emphasize the identical slope at high K^+ activity. The horizontal dashed line was added to highlight the sub-Nernstian response region of curve C.